International Journal of Fracture **75**: 49–67, 1996.

Growth behavior of internal delaminations in composite beam/plates under compression: effect of the end conditions

G.A. KARDOMATEAS and A.A. PELEGRI
School of Aerospace Engineering, Georgia Institute of Technology, Atlanta, Georgia 30332-0150, USA

Received 9 December 1994; accepted in revised form 30 July 1995

Abstract. The effect of the end conditions, i.e. clamped-clamped vs. simply-supported ends on the initial postbuckling and growth behavior of delaminations in plates is studied. The study does not impose any restrictive assumptions regarding the delamination thickness and plate length. First, a closed form solution for the mode mixity, energy release rate and deformation quantities is derived for the case of a clamped-clamped delaminated plate, which complements the already existing solution for a delaminated simply-supported plate. A perturbation procedure is followed, which is based on an asymptotic expansion of the load and deformation quantities in terms of the distortion parameter of the delaminated layer, the latter being considered a compressive elastica. The additional complication in the clamped-clamped case arises because now the amplitude at the clamped end needs to be expanded in terms of the distortion parameter of the delaminated part, in addition to the amplitude at the common section and the distortion parameter of the base plate. The effects of the end conditions on the growth behavior are found to depend on the relative location of the delamination through the thickness. For the same plate length and thickness and the same delamination length and applied strain, delaminations located closer to the surface exhibit nearly the same energy release rate and mode mixity either in a clamped-clamped or a simply supported configuration. However, in delaminations located further away from the surface, for the same applied strain, the energy release rate is larger and there is also a higher mode II component in the simply-supported case. Moreover, the mid-point transverse displacement of the delaminated layer as well as that of the substrate part, is larger in the simply supported case. The same major trend that has been observed in the simply supported case, i.e. the increased growth resistance of the delaminations located near the surface relative to the ones located further inside the plate, is also observed in the clamped-clamped case.

1. Introduction

Fiber reinforced composites are widely used in aircraft structures due to their high specific strength. Composite plates can be made by bonding individual layers containing unidirectional fibers. Low-velocity impacts and manufacturing defects lead to local debonding, which has been referred to as delamination. These are essentially interface cracks. In the presence of delaminations, these materials may work well under tension; in the zones of compression, however, delamination buckling can occur. As a consequence, structural elements with delaminations under compression suffer a degradation of their stiffness and buckling strength and potential loss of integrity from possible growth of the interlayer crack. Besides strength, delaminations can influence other performance characteristics, such as the energy absorption capacity of composite beam systems [1].

Delamination buckling in plates under compression has received considerable attention and numerous contributions have addressed related issues in both one-dimensional and two-dimensional treatments, e.g. [2–7]. However, although the critical point can be fairly well determined and has been extensively studied, limited work has focused on the postbuckling behavior, which ultimately governs the growth characteristics of the delamination.

Chai, Babcock and Knauss [2] presented a one-dimensional model by assuming essentially a delamination in an infinitely thick plate. In this model, which has also been called the 'thin film' model, the unbuckled (base) plate is assumed to be subject to a uniform compressive strain. In the general case, the finite plate length and thickness is expected to influence the bifurcation point and post-critical behavior of the delamination and subsequently its growth characteristics. An additional influence may also arise from the end fixity conditions of the base plate. To this extent, Simitses et al. [3] studied the critical load for a delamination of arbitrary thickness and size in a finite plate; their results showed a range of critical load vs. thin film load ratios, depending on delamination and base plate dimensions, as well as base plate end fixity (simply-supported vs. clamped). Concerning the post-critical behavior of delaminations of arbitrary size, Kardomateas [8] provided a formulation for studying the postbuckling behavior by using elastica theory for representing the deflections of the buckled layer; this work resulted in a system of nonlinear equations rather than closed form expressions. The post-critical behavior was also studied by Sheinman and Adan [9] through a high-order kinematic model, with the nonlinear differential equations solved by Newton's method and a special finite-difference scheme.

In a recent paper, Kardomateas [10] studied the initial postbuckling behavior of general delaminated composites (i.e. with no restrictive assumptions on the delamination dimensions) by using a perturbation procedure based on an asymptotic expansion of the load and deformation quantities in terms of the distortion parameter of the delaminated layer, the latter being considered a compressive elastica. The analysis lead to closed form solutions for the load versus applied compressive displacement and the near tip resultant moments and forces. This work assumed simply supported ends because the value of the amplitude variable at the supported end is fixed and this simplifies the analysis.

The growth behavior for the simply-supported case was studied by employing the bimaterial interface crack solutions for the mode mixity and the energy release rate in terms of the resultant moments and forces, as derived by Suo and Hutchinson [11]. These relations are actually simplified because the material is assumed homogeneous. The same relations are used in the present study for the clamped-clamped case since once the initial postbuckling behavior is determined the resultant moments and forces at the common section are known.

The formulation presented hereby is a closed form solution, hence results can be produced for a variety of configurations with minimum effort. Alternative numerical (finite element) strategies have been pursued to investigate buckling induced delamination growth such as by Nilsson and Storåkers [12]. These detailed finite element studies can provide answers to some of the more complex questions, such as the effect of a general anisotropy (rather than pure orthotropy), and possible contact effects that may arise after large amounts of growth and applied strain, and which cannot be handled by the present formulation. Moreover, they can be used to solve the more complex two-dimensional configurations. A numerical study such as that by Nilsson and Storåkers [12] could also provide improved estimates for the delamination tip stress intensity factors by relaxing the restrictive assumptions in the interface crack solutions of Hutchinson and Suo [13], which are asymptotic ones for semi-infinite cracks.

Hence, in this paper, the initial postbuckling behavior of clamped-clamped delaminated composites (with no restrictive assumptions on the delamination dimensions) is studied by using a perturbation procedure based on an asymptotic expansion of the load and deformation quantities in terms of the distortion parameter of the delaminated layer, the latter being considered a compressive elastica. The additional complication in the clamped-clamped case

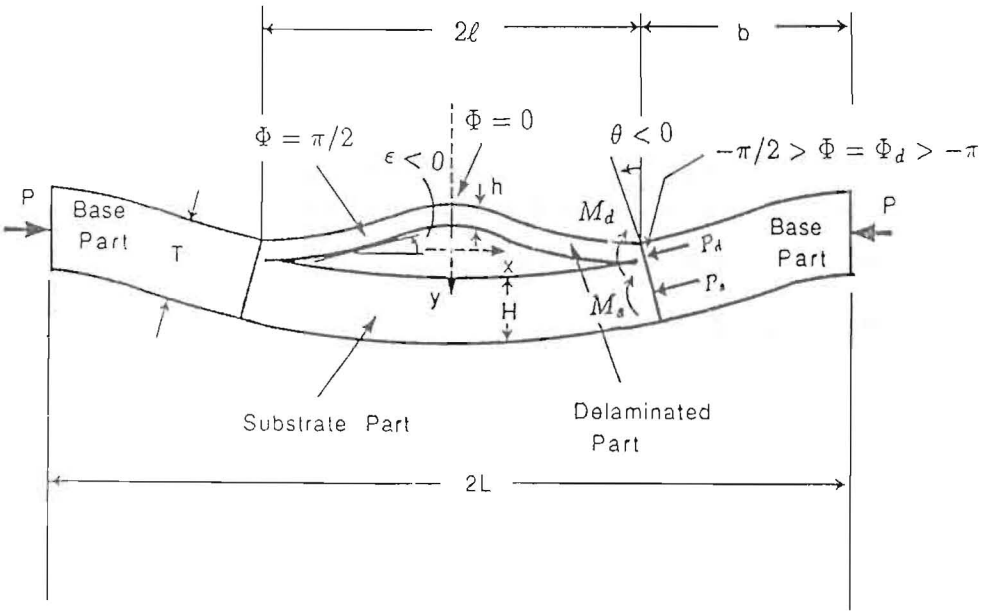

Figure 1. Definition of the geometry. A clamped-clamped delaminated beam/plate.

relative to the simply-supported case arises because now not only the amplitude at the common section, but also the amplitude at the clamped end, as well as the distortion paremeter of the base plate, need to be expanded in terms of the distortion parameter of the delaminated part. This is because the value of the amplitude variable at the clamped end has no longer a constant, fixed value; it is rather set by the zero slope condition at this end.

The present analysis will lead to closed form solutions for the load versus applied compressive displacement and the near tip resultant moments and forces. Subsequently, the bimaterial interface crack solutions for the energy release rate and the mode mixity in terms of the resultant moments and forces, as derived in [11] will be employed to study the growth characteristics of the delamination in the clamped-clamped case. Results for the growth characteristics for a range of relative delamination thicknesses will be produced and compared with the corresponding ones for the simply-supported case.

2. The initial postbuckling behavior for clamped ends

Referring to Figure 1, consider a plate of half-length L (and unit width) with a through-the-width delamination of half-length ℓ, symmetrically located. The delamination is at an arbitrary position through the thickness T. Over the delaminated region, the laminate consists of the part above the delamination, of thickness h referred to as the 'delaminated' part, and the part below the delamination, of thickness $H = T - h$, referred to as the 'substrate' part. The remaining, intact laminate, of thickness T and length $b = L - \ell$, is referred to as the 'base' plate. Accordingly, the subscript $i = d, s, b$ refers to the delaminated part, the substrate or the base plate, respectively.

The solution in [10] is based on considering the buckled configuration of the delaminated layer as part of an inflectional elastica with end amplitude Φ_d and distortion parameter ε. At

the critical state, the end amplitude is Φ_d^0. Suppose that in the slightly buckled configuration, Φ_d can be expanded in the form:

$$\Phi_d = \Phi_d^0 + \phi_d^{(1)}\varepsilon + \phi_d^{(2)}\varepsilon^2 + \mathrm{O}(\varepsilon^3). \tag{1}$$

Then the end rotation at the common section θ is given by expanding the relevant expression [14] in Taylor series in terms of ε (notice that at the critical state $\theta^0 = 0$)

$$\begin{aligned}\theta &= (\sin\Phi_d)\varepsilon - \tfrac{1}{24}(\sin\Phi_d\cos^2\Phi_d)\varepsilon^3 + \cdots \\ &= (\sin\Phi_d^0)\varepsilon + (\cos\Phi_d^0)\phi_d^{(1)}\varepsilon^2 \\ &\quad + \left[(\cos\Phi_d^0)\phi_d^{(2)} - (\sin\Phi_d^0)\frac{\phi_d^{(1)2}}{2} - \tfrac{1}{24}\sin\Phi_d^0\cos^2\Phi_d^0\right]\varepsilon^3 + \cdots \\ &= \theta^{(1)}\varepsilon + \theta^{(2)}\varepsilon^2 + \theta^{(3)}\varepsilon^3 + \mathrm{O}(\varepsilon^4).\end{aligned} \tag{2}$$

Due to the continuity condition, θ is the same for both the delaminated and substrate parts as well as the base plate.

The asymptotic expansion for the end moment M_d is similarly found by substituting (1) into the relevant expression [14] and subsequently expanding in Taylor series (again $M_d^0 = 0$):

$$\begin{aligned}\frac{\ell M_d}{D_d} &= (\Phi_d\cos\Phi_d)\varepsilon + \frac{\Phi_d}{16}\left(\frac{1}{3} - \frac{\sin 2\Phi_d}{2\Phi_d}\right)(\cos\Phi_d)\varepsilon^3 + \cdots \\ &= \frac{\ell}{D_d}\left(M_d^{(1)}\varepsilon + M_d^{(2)}\varepsilon^2 + M_d^{(3)}\varepsilon^3\right) + \mathrm{O}(\varepsilon^4),\end{aligned} \tag{3a}$$

where $D_d = Eh^3/\left[12\left(1-\nu^2\right)\right]$, is the bending stiffness, and

$$\frac{\ell M_d^{(1)}}{D_d} = \Phi_d^0\cos\Phi_d^0; \qquad \frac{\ell M_d^{(2)}}{D_d} = (\cos\Phi_d^0 - \Phi_d^0\sin\Phi_d^0)\phi_d^{(1)}, \tag{3b}$$

$$\begin{aligned}\frac{\ell M_d^{(3)}}{D_d} &= (\cos\Phi_d^0 - \Phi_d^0\sin\Phi_d^0)\phi_d^{(2)} - \left(\sin\Phi_d^0 + \frac{\Phi_d^0}{2}\cos\Phi_d^0\right)\phi_d^{(1)2} \\ &\quad + \frac{\Phi_d^0}{16}\left(\frac{1}{3} - \frac{\sin 2\Phi_d^0}{2\Phi_d^0}\right)(\cos\Phi_d^0).\end{aligned} \tag{3c}$$

Likewise, the axial force P_d and the flexural contraction f_d can be found in an asymptotic expansion form.

Although the substrate part and the base plate undergo moderate bending with no inflection point, we may also use the elastica theory to describe their (nonlinear) deformation; in this case the inflection points are outside the actual elastic curve. For the substrate part, we have to expand not only the amplitude Φ_s, but also the distortion parameter α_s in a perturbation series with respect to the distortion parameter of the delaminated layer ε

$$\Phi_s = \Phi_s^0 + \phi_s^{(1)}\varepsilon + \phi_s^{(2)}\varepsilon^2 + \mathrm{O}(\varepsilon^3), \tag{4a}$$

$$\alpha_s = \alpha_s^{(1)}\varepsilon + \alpha_s^{(2)}\varepsilon^2 + \alpha_s^{(3)}\varepsilon^3 + \mathrm{O}(\varepsilon^4). \tag{4b}$$

The base plate in this previous work [10] was assumed to be simply supported, so at the simply-supported end, the amplitude $\Phi = \Phi_e = -\pi/2$, and at the common section $\Phi = \Phi_b$. The amplitude at the common section, Φ_b and the distortion paremeter of the base plate α_b were expanded in terms of the distortion parameter of the delaminated part ε. This simplifies the problem considerably and for this reason the assumption of simply-supported ends was adopted in the initial work of Kardomateas [10]. However, for a clamped end, Φ_e is determined by the condition of zero slope, which introduces an additional complication in the problem formulation, in the sense that Φ_e should now also admit an asymptotic expansion.

Therefore, not only the amplitude at the common section Φ_b, but also the amplitude at the clamped end Φ_e, as well as the distortion parameter of the base plate, α_b, are now expanded in terms of the distortion parameter of the delaminated part ε

$$\Phi_b = \Phi_b^0 + \phi_b^{(1)}\varepsilon + \phi_b^{(2)}\varepsilon^2 + \mathrm{O}(\varepsilon^3), \tag{5a}$$

$$\Phi_e = \Phi_e^0 + \phi_e^{(1)}\varepsilon + \phi_e^{(2)}\varepsilon^2 + \mathrm{O}(\varepsilon^3), \tag{5b}$$

$$\alpha_b = \alpha_b^{(1)}\varepsilon + \alpha_b^{(2)}\varepsilon^2 + \alpha_b^{(3)}\varepsilon^3 + \mathrm{O}(\varepsilon^4). \tag{5c}$$

The rotation at either the common section θ_b or the end θ_e is given by expanding the relevant expression for the slope from Britvek [14] in Taylor series in terms of the distortion parameter of the base plate α_b as follows:

$$\begin{aligned}\theta_i &= \left(\sin\Phi_i + \frac{\cos\Phi_b - \cos\Phi_e}{\Phi_b - \Phi_e}\right)\alpha_b + R(\Phi_i)\alpha_b^3 + \cdots \\ &= \theta_i^{(1)}\varepsilon + \theta_i^{(2)}\varepsilon^2 + \theta_i^{(3)}\varepsilon^3 + \mathrm{O}(\varepsilon^4), \quad i = b, e,\end{aligned} \tag{6a}$$

where $R(\Phi_i)$ is defined by

$$\begin{aligned}R(\Phi_i) = {} & \frac{7}{48}\frac{\cos\Phi_b - \cos\Phi_e}{\Phi_b - \Phi_e} - \frac{3}{32}\frac{\cos\Phi_b - \cos\Phi_e}{(\Phi_b - \Phi_e)^2}(\sin 2\Phi_b - \sin 2\Phi_e) \\ & -\frac{1}{3}\left(\frac{\cos\Phi_b - \cos\Phi_e}{\Phi_b - \Phi_e}\right)^3 - \tfrac{1}{24}\sin\Phi_i^0\cos^2\Phi_i^0.\end{aligned} \tag{6b}$$

Substituting (5) into (6) gives explicit expressions for the $\theta_i^{(1)}$, $\theta_i^{(2)}$, $\theta_i^{(3)}$, etc. It is helpful to define the quantities β_b, β_e, as follows

$$\beta_i = \sin\Phi_i^0 + \frac{\cos\Phi_b^0 - \cos\Phi_e^0}{\Phi_b^0 - \Phi_e^0}, \quad i = b, e, \tag{7a}$$

Also define ξ_b and ξ_e, by

$$\xi_b = \frac{\beta_b}{\Phi_b^0 - \Phi_e^0} - \frac{\cos\Phi_b^0}{2}; \qquad \xi_e = \frac{\beta_e}{\Phi_b^0 - \Phi_e^0} + \frac{\cos\Phi_e^0}{2}, \tag{7b}$$

Then the first order rotations are

$$\theta_i^{(1)} = \beta_i\alpha_b^{(1)}, \quad i = b, e, \tag{8a}$$

and the second order rotations are

$$\theta_i^{(2)} = \left[(\cos\Phi_i^0)\phi_i^{(1)} + \frac{\beta_e\phi_e^{(1)} - \beta_b\phi_b^{(1)}}{\Phi_b^0 - \Phi_e^0}\right]\alpha_b^{(1)} + \beta_i\alpha_b^{(2)}, \quad i = b, e. \tag{8b}$$

After some algebraic manipulation, the third order rotation at the common section is found as follows

$$\begin{aligned}\theta_i^{(3)} = &\left[(\cos\Phi_i^0)\phi_i^{(2)} + \frac{\beta_e\phi_e^{(2)} - \beta_b\phi_b^{(2)}}{\Phi_b^0 - \Phi_e^0} - (\sin\Phi_i^0)\frac{\phi_i^{(1)2}}{2} - \right.\\ &\left. - \frac{\beta_b + \beta_e}{(\Phi_b^0 - \Phi_e^0)^2}\phi_b^{(1)}\phi_e^{(1)} + \frac{\xi_e\phi_e^{(1)2} + \xi_b\phi_b^{(1)2}}{(\Phi_b^0 - \Phi_e^0)}\right]\alpha_b^{(1)}\\ &+ \left[(\cos\Phi_i^0)\phi_i^{(1)} + \frac{\beta_e\phi_e^{(1)} - \beta_b\phi_b^{(1)}}{\Phi_b^0 - \Phi_e^0}\right]\alpha_b^{(2)} + \beta_i\alpha_b^{(3)} + R(\Phi_i^0)\alpha_b^{(1)3},\\ &i = b, e.\end{aligned} \tag{8c}$$

Concerning the end moment M_b, Britvek [14] gives the following expression

$$\begin{aligned}\frac{bM_b}{D_b} = &(\Phi_b - \Phi_e)(\cos\Phi_b)\alpha_b\\ &+\tfrac{1}{16}(\Phi_b - \Phi_e)\left(\frac{1}{3} - \frac{1}{2}\frac{\sin 2\Phi_b - \sin 2\Phi_e}{\Phi_b - \Phi_e}\right)(\cos\Phi_b)\alpha_b^3 + \cdots.\end{aligned} \tag{9a}$$

For convenience, define

$$q = \cos\Phi_b^0 - \left(\Phi_b^0 - \Phi_e^0\right)\sin\Phi_b^0, \tag{9b}$$

then use of (5) gives the following asymptotic expansion (again $M_b^0 = 0$)

$$\frac{bM_b}{D_b} = \frac{b}{D_b}\left(M_b^{(1)}\varepsilon + M_b^{(2)}\varepsilon^2 + M_b^{(3)}\varepsilon^3\right) + \mathrm{O}(\varepsilon^4), \tag{9c}$$

where

$$\frac{bM_b^{(1)}}{D_b} = \left(\Phi_b^0 - \Phi_e^0\right)(\cos\Phi_b^0)\alpha_b^{(1)}, \tag{9d}$$

$$\frac{bM_b^{(2)}}{D_b} = \left[q\phi_b^{(1)} - (\cos\Phi_b^0)\phi_e^{(1)}\right]\alpha_b^{(1)} + \left(\Phi_b^0 - \Phi_e^0\right)(\cos\Phi_b^0)\alpha_b^{(2)}, \tag{9e}$$

and the third order moment is

$$\begin{aligned}\frac{bM_b^{(3)}}{D_b} = &\left(\Phi_b^0 - \Phi_e^0\right)(\cos\Phi_b^0)\alpha_b^{(3)} + \left[q\phi_b^{(1)} - (\cos\Phi_b^0)\phi_e^{(1)}\right]\alpha_b^{(2)}\\ &+ \left[q\phi_b^{(2)} - (\cos\Phi_b^0)\phi_e^{(2)} - \phi_b^{(1)}\left(\phi_b^{(1)} - \phi_e^{(1)}\right)\sin\Phi_b^0\right.\\ &\left. - \left(\Phi_b^0 - \Phi_e^0\right)(\cos\Phi_b^0)\frac{\phi_b^{(1)2}}{2}\right]\alpha_b^{(1)}\\ &+\tfrac{1}{16}(\Phi_b^0 - \Phi_e^0)\left(\frac{1}{3} - \frac{1}{2}\frac{\sin 2\Phi_b^0 - \sin 2\Phi_e^0}{\Phi_b^0 - \Phi_e^0}\right)(\cos\Phi_b^0)\alpha_b^{(1)3}.\end{aligned} \tag{9f}$$

Likewise, the axial force at the base plate (which is also the applied force) is given by

$$\frac{b^2P}{D_b} = (\Phi_b - \Phi_e)^2 + (\Phi_b - \Phi_e)^2 \times \left[\frac{1}{8} - \frac{1}{16}\frac{\sin 2\Phi_b - \sin 2\Phi_e}{\Phi_b - \Phi_e} - \frac{1}{2}\left(\frac{\cos\Phi_b - \cos\Phi_e}{\Phi_b - \Phi_e}\right)^2\right]\alpha_b^2$$

$$= \frac{b^2}{D_b}\left(P^0 + P^{(1)}\varepsilon + P^{(2)}\varepsilon^2\right) + O(\varepsilon^3), \tag{10a}$$

where

$$\frac{b^2P^0}{D_b} = \left(\Phi_b^0 - \Phi_e^0\right)^2; \qquad \frac{b^2P^{(1)}}{D_b} = 2\left(\Phi_b^0 - \Phi_e^0\right)\left(\phi_b^{(1)} - \phi_e^{(1)}\right), \tag{10b}$$

and the second order force is

$$\frac{b^2P^{(2)}}{D_b} = \left(\phi_b^{(1)} - \phi_e^{(1)}\right)^2 + 2\left(\Phi_b^0 - \Phi_e^0\right)\left(\phi_b^{(2)} - \phi_e^{(2)}\right) + \left(\Phi_b^0 - \Phi_e^0\right)^2\left[\frac{1}{8} - \frac{1}{16}\frac{\sin 2\Phi_b^0 - \sin 2\Phi_e^0}{\Phi_b^0 - \Phi_e^0} - \frac{1}{2}\left(\frac{\cos\Phi_b^0 - \cos\Phi_e^0}{\Phi_b^0 - \Phi_e^0}\right)^2\right]\alpha_b^{(1)2}. \tag{10c}$$

Finally, the flexural contraction f_b between the clamped end and the common section is

$$f_b = \frac{b}{4}\left[1 - \frac{1}{2}\frac{\sin 2\Phi_b - \sin 2\Phi_e}{\Phi_b - \Phi_e} - 2\left(\frac{\cos\Phi_b - \cos\Phi_e}{\Phi_b - \Phi_e}\right)^2\right]\alpha_b^2 + \cdots$$

$$= f_b^{(2)}\varepsilon^2 + O(\varepsilon^3), \tag{11a}$$

where

$$f_b^{(2)} = \frac{b}{4}\left[1 - \frac{1}{2}\frac{\sin 2\Phi_b^0 - \sin 2\Phi_e^0}{\Phi_b^0 - \Phi_e^0} - 2\left(\frac{\cos\Phi_b^0 - \cos\Phi_e^0}{\Phi_b^0 - \Phi_e^0}\right)^2\right]\alpha_b^{(1)2}. \tag{11b}$$

Therefore, in the case of clamped ends, additional quantities to be determined (versus the simply-supported case) are the Φ_e^0, $\phi_e^{(1)}$ and $\phi_e^{(2)}$.

Having obtained the asymptotic expressions for the force and deformation quantities, we shall discuss the formulation of the equilibrium and compatibility requirements that will ultimately define the nonlinear post-critical path. Force and moment equilibrium at the common section require

$$P_d + P_s - P = 0, \tag{12a}$$

$$M_d + M_s + M_b - P_d\frac{H}{2} + P_s\frac{h}{2} = 0. \tag{12b}$$

The deflections of the delaminated and substrate parts should be geometrically compatible. Thus, a second condition necessary for a solution involves the compatible shortening of the delaminated and substrate parts, which consist, in turn, of the compressive and flexural shortening

$$\left(f_d + 2\frac{P_d \ell}{Eh}\right) - \left(f_s + 2\frac{P_s \ell}{EH}\right) + \theta T = 0. \tag{13}$$

As the compressive load P is applied, the plate remains flat and a primary state solution (pure compression) is characterized by $P^0 = P_d^0 T/h$ and $P_s^0 = P_d^0 H/h$, which gives from (10b)

$$\Phi_s^0 = \Phi_d^0 \sqrt{\frac{D_d H}{D_s h}}, \tag{14a}$$

$$\Phi_b^0 - \Phi_e^0 = -\Phi_d^0 \frac{b}{\ell}\sqrt{\frac{D_d T}{D_b h}}. \tag{14b}$$

Moreover, the first order zero slope at the clamped end $\theta_e^{(1)} = 0$ gives from (8a):

$$\beta_e = \sin\Phi_e^0 + \frac{\cos\Phi_b^0 - \cos\Phi_e^0}{\Phi_b^0 - \Phi_e^0} = 0. \tag{14c}$$

Although determination of the critical point is not a primary objective of this paper and the buckling analysis has been thoroughly carried out in other works, e.g. [3], we shall briefly describe the equations for the critical point (in terms of Φ_d^0) for the sake of completeness, and because the formulation for the initial postbuckling naturally follows that for the critical point.

By equating the first order rotation at the common section, we obtain $\alpha_s^{(1)}$ and $\alpha_b^{(1)}$

$$\alpha_s^{(1)} = \frac{\sin\Phi_d^0}{\sin\Phi_s^0}; \qquad \alpha_b^{(1)} = \frac{\sin\Phi_d^0}{\beta_b}. \tag{14d}$$

Writing the moment equilibrium (12b) and the geometric compatibility (13) for the first order terms, and eliminating the quantity $\left[P_d^{(1)} H - P_s^{(1)} h\right]$ leads to the characteristic equation, for the determination of Φ_d^0

$$\frac{D_d}{\ell}\Phi_d^0 \cos\Phi_d^0 + \sin\Phi_d^0 \left[\frac{D_s}{\ell}\Phi_s^0 \cot\Phi_s^0 + \frac{D_b}{b}\left(\Phi_b^0 - \Phi_e^0\right)\frac{\cos\Phi_b^0}{\beta_b} + \frac{ETHh}{4\ell}\right] = 0. \tag{14e}$$

Equations (14c) and (14e) constitute a system of two nonlinear equations in Φ_d^0 and Φ_b^0. Notice that Φ_s^0 and Φ_e^0 are determined in terms of Φ_d^0 and Φ_b^0 by use of (14a,b). These two nonlinear algebraic equations were solved by using Powell's method [15].

Next, the initial postbuckling behavior for the clamped case is considered.

2.1. First order forces

Determination of the first order forces requires determining the five quantities $\phi_d^{(1)}$, $\phi_s^{(1)}$, $\phi_b^{(1)}$, $\phi_e^{(1)}$ and $\alpha_b^{(2)}$.

Force equilibrium, (12a) for the first order terms, i.e.,

$$P_d^{(1)} + P_s^{(1)} = P^{(1)},$$

and use of the expressions for the first order forces (the expressions for $P_d^{(1)}$ and $P_s^{(1)}$ are given in [10] and the expression for $P^{(1)}$ is (10b)) gives one equation

$$\frac{\Phi_d^0}{\Phi_b^0 - \Phi_e^0}\frac{D_d b^2}{D_b \ell^2}\phi_d^{(1)} + \frac{\Phi_s^0}{\Phi_b^0 - \Phi_e^0}\frac{D_s b^2}{D_b \ell^2}\phi_s^{(1)} + \phi_e^{(1)} - \phi_b^{(1)} = 0. \tag{15a}$$

A second equation is obtained by the condition of end fixity

$$\theta_e^{(2)} = 0,$$

and by use of (8b), as follows

$$\left[\left(\cos\Phi_e^0 + \frac{\beta_e}{\Phi_b^0 - \Phi_e^0}\right)\phi_e^{(1)} - \frac{\beta_b}{\Phi_b^0 - \Phi_e^0}\phi_b^{(1)}\right]\alpha_b^{(1)} + \beta_e\alpha_b^{(2)} = 0. \tag{15b}$$

By equating the second order terms in the expressions for the slope at the common section $\theta_b^{(2)}$ (8b) and that of $\theta_d^{(2)}$ (which is given in [10]) we can find the third equation as follows

$$-(\cos\Phi_d^0)\phi_d^{(1)} + \left[\frac{\beta_e}{\Phi_b^0 - \Phi_e^0}\phi_e^{(1)} + \left(\cos\Phi_b^0 - \frac{\beta_b}{\Phi_b^0 - \Phi_e^0}\right)\phi_b^{(1)}\right]\alpha_b^{(1)} + \beta_b\alpha_b^{(2)} = 0. \tag{15c}$$

Furthermore, by equating the slope from the delaminated layer and the substrate at the common section, we can find an expression for $\alpha_s^{(2)}$ in terms of $\phi_d^{(1)}$ and $\phi_s^{(1)}$ in the form

$$\alpha_s^{(2)} = \gamma_d\phi_d^{(1)} + \gamma_s\phi_s^{(1)}, \tag{16a}$$

where

$$\gamma_d = \frac{\cos\Phi_d^0}{\sin\Phi_s^0}; \qquad \gamma_s = -\frac{(\cos\Phi_s^0)}{\sin\Phi_s^0}\alpha_s^{(1)}. \tag{16b}$$

Next, the moment equilibrium (12b) for the second order terms is

$$M_d^{(2)} + M_s^{(2)} + M_b^{(2)} = \tfrac{1}{2}\left[P_d^{(2)}H - P_s^{(2)}h\right]. \tag{16c}$$

The geometric compatibility (13) for the second order terms gives

$$f_d^{(2)} - f_s^{(2)} + \theta^{(2)}T = \left[P_s^{(2)}h - P_d^{(2)}H\right]\frac{2\ell}{EhH}. \tag{16d}$$

Eliminating the quantity $\left[P_s^{(2)}h - P_d^{(2)}H\right]$ from (16c) and (16d) gives the following fourth linear equation

$$a_{11}\phi_d^{(1)} + a_{12}\phi_s^{(1)} + \frac{D_b}{b}\left[-(\cos\Phi_b^0)\alpha_b^{(1)}\phi_e^{(1)} + q\alpha_b^{(1)}\phi_b^{(1)} + \left(\Phi_b^0 - \Phi_e^0\right)(\cos\Phi_b^0)\alpha_b^{(2)}\right]$$
$$= \left[\frac{\ell}{2}\left(1 - \frac{\sin 2\Phi_s^0}{2\Phi_s^0}\right)\alpha_s^{(1)2} - \frac{\ell}{2}\left(1 - \frac{\sin 2\Phi_d^0}{2\Phi_d^0}\right)\right]\frac{EhH}{4\ell}, \tag{17a}$$

where

$$a_{11} = \frac{D_d}{\ell}(\cos\Phi_d^0 - \Phi_d^0 \sin\Phi_d^0) + \frac{D_s}{\ell}\Phi_s^0(\cos\Phi_s^0)\gamma_d + (\cos\Phi_d^0)\frac{EhHT}{4\ell}, \tag{17b}$$

$$a_{12} = \frac{D_s}{\ell}\left[(\cos\Phi_s^0 - \Phi_s^0 \sin\Phi_s^0)\alpha_s^{(1)} + \Phi_s^0(\cos\Phi_s^0)\gamma_s\right]. \tag{17c}$$

The fifth linear equation needed to find $\phi_d^{(1)}$, $\phi_s^{(1)}$, $\phi_e^{(1)}$, $\phi_b^{(1)}$ and $\alpha_b^{(2)}$ is the first order geometric compatibility (13) at the common section, which becomes after the expressions for the first order delamination and substrate forces, and for the first order rotation (these are given in [10]) are substituted

$$-\frac{D_d}{\ell^2}\Phi_d^0 H\phi_d^{(1)} + \frac{D_s}{\ell^2}\Phi_s^0 h\phi_s^{(1)} = \frac{EhHT}{4\ell}\sin\Phi_d^0. \tag{17d}$$

The foregoing system of five linear equations, (15a,b,c) and (17a,d), allows finding $\phi_d^{(1)}$, $\phi_s^{(1)}$, $\phi_b^{(1)}$, $\phi_e^{(1)}$ and $\alpha_b^{(2)}$ hence the first order forces $P_d^{(1)}$, $P_s^{(1)}$ and the first order applied force $P^{(1)} = P_d^{(1)} + P_s^{(1)}$.

2.2. Second order forces

For the second order forces, a procedure similar to the first order leads to five linear algebraic equations for $\phi_d^{(2)}$, $\phi_s^{(2)}$, $\phi_e^{(2)}$, $\phi_b^{(2)}$ and $\alpha_b^{(3)}$. In particular, a second order force equilibrium (12a)

$$P_d^{(2)} + P_s^{(2)} = P^{(2)},$$

together with (10c) for $P^{(2)}$ and the corresponding expressions for $P_d^{(2)}$ and $P_s^{(2)}$ from [10], gives one linear equation

$$\begin{aligned}
&\frac{D_d b^2}{D_b \ell^2}\Phi_d^0\phi_d^{(2)} + \frac{D_s b^2}{D_b \ell^2}\Phi_s^0\phi_s^{(2)} + \left(\Phi_b^0 - \Phi_e^0\right)\left(\phi_e^{(2)} - \phi_b^{(2)}\right) \\
&\quad = \frac{\left(\phi_b^{(1)} - \phi_e^{(1)}\right)^2}{2} + \left(\frac{\Phi_b^0 - \Phi_e^0}{2}\right)^2 \\
&\qquad \times \left[\frac{1}{4} - \frac{1}{8}\frac{\sin 2\Phi_b^0 - \sin 2\Phi_e^0}{\Phi_b^0 - \Phi_e^0} - \left(\frac{\cos\Phi_b^0 - \cos\Phi_e^0}{\Phi_b^0 - \Phi_e^0}\right)^2\right]\alpha_b^{(1)2} \\
&\qquad - \frac{D_d b^2}{2D_b \ell^2}\left[\phi_d^{(1)2} + \frac{\Phi_d^{02}}{8}\left(1 - \frac{\sin 2\Phi_d^0}{2\Phi_d^0}\right)\right] \\
&\qquad - \frac{D_s b^2}{2D_b \ell^2}\left[\phi_s^{(1)2} + \frac{\Phi_s^{02}}{8}\left(1 - \frac{\sin 2\Phi_s^0}{2\Phi_s^0}\right)\alpha_s^{(1)2}\right].
\end{aligned} \tag{18a}$$

A second equation is obtained from the condition of end fixity, i.e.

$$\theta_e^{(3)} = 0,$$

which, by use of (8c), gives

$$\left(\cos\Phi_e^0+\frac{\beta_e}{\Phi_b^0-\Phi_e^0}\right)\alpha_b^{(1)}\phi_e^{(2)}-\frac{\beta_b}{\Phi_b^0-\Phi_e^0}\alpha_b^{(1)}\phi_b^{(2)}+\beta_e\alpha_b^{(3)}$$
$$=\left[\frac{\beta_b+\beta_e}{(\Phi_b^0-\Phi_e^0)^2}\phi_b^{(1)}\phi_e^{(1)}+(\sin\Phi_e^0)\frac{\phi_e^{(1)2}}{2}-\frac{\xi_e\phi_e^{(1)2}+\xi_b\phi_b^{(1)2}}{(\Phi_b^0-\Phi_e^0)}\right]\alpha_b^{(1)}$$
$$+\left[\frac{\beta_b\phi_b^{(1)}-\beta_e\phi_e^{(1)}}{\Phi_b^0-\Phi_e^0}-(\cos\Phi_e^0)\phi_e^{(1)}\right]\alpha_b^{(2)}-R(\Phi_e^0)\alpha_b^{(1)3}. \tag{18b}$$

By equating the third order terms in the expressions for the slope at the common section for the delaminated and the substrate parts, $\theta^{(3)}$ (these are given in [10]), we can find $\alpha_s^{(3)}$:

$$\alpha_s^{(3)}=\gamma_d\phi_d^{(2)}+\gamma_s\phi_s^{(2)}+\gamma_c, \tag{19a}$$

where γ_d, γ_s are, as in (16b), and γ_c is given in terms of the following quantities

$$\psi_d=-\left(\frac{\phi_d^{(1)2}}{2}+\frac{1}{24}\cos^2\Phi_d^0\right)\sin\Phi_d^0, \tag{19b}$$

$$\psi_s=-\left(\frac{\phi_s^{(1)2}}{2}+\frac{1}{24}\alpha_s^{(1)2}\cos^2\Phi_s^0\right)\alpha_s^{(1)}\sin\Phi_s^0+\phi_s^{(1)}\alpha_s^{(2)}\cos\Phi_s^0, \tag{19c}$$

as follows

$$\gamma_c=\frac{\psi_d-\psi_s}{\sin\Phi_s^0}. \tag{19d}$$

Moreover, in a similar fashion to the first order forces, by equating the third order terms in the expressions for the slope at the common section for the delaminated and the base parts $\theta_d^{(3)}=\theta_b^{(3)}$ and using (8c) we obtain a third equation as follows

$$-(\cos\Phi_d^0)\phi_d^{(2)}+\frac{\beta_e}{\Phi_b^0-\Phi_e^0}\alpha_b^{(1)}\phi_e^{(2)}+\left(\cos\Phi_b^0-\frac{\beta_b}{\Phi_b^0-\Phi_e^0}\right)\alpha_b^{(1)}\phi_b^{(2)}+\beta_b\alpha_b^{(3)}$$
$$=\left[\frac{\beta_b+\beta_e}{(\Phi_b^0-\Phi_e^0)^2}\phi_b^{(1)}\phi_e^{(1)}+(\sin\Phi_b^0)\frac{\phi_b^{(1)2}}{2}-\frac{\xi_e\phi_e^{(1)2}+\xi_b\phi_b^{(1)2}}{(\Phi_b^0-\Phi_e^0)}\right]\alpha_b^{(1)}$$
$$-\left[(\cos\Phi_b^0)\phi_b^{(1)}+\frac{\beta_e\phi_e^{(1)}-\beta_b\phi_b^{(1)}}{\Phi_b^0-\Phi_e^0}\right]\alpha_b^{(2)}-R(\Phi_b^0)\alpha_b^{(1)3}$$
$$-\sin\Phi_d^0\left(\frac{\phi_d^{(1)2}}{2}+\frac{\cos^2\Phi_d^0}{24}\right), \tag{20a}$$

Now the moment equilibrium equation (12b) for the third order terms is

$$M_d^{(3)}+M_s^{(3)}+M_b^{(3)}=\tfrac{1}{2}\left[P_d^{(3)}H-P_s^{(3)}h\right]. \tag{20b}$$

The geometric compatibility (13) for the third order terms gives

$$f_d^{(3)} - f_s^{(3)} + \theta^{(3)} T = \left[P_s^{(3)} h - P_d^{(3)} H \right] \frac{2\ell}{EhH}. \tag{20c}$$

Eliminating now the quantity $\left[P_s^{(3)} h - P_d^{(3)} H \right]$ from (20b,c) gives the following fourth linear equation for $\phi_d^{(2)}$ and $\phi_s^{(2)}$

$$a_{11}\phi_d^{(2)} + a_{12}\phi_s^{(2)} + \frac{D_b}{b}\left[-(\cos\Phi_b^0)\alpha_b^{(1)}\phi_e^{(2)} + q\alpha_b^{(1)}\phi_b^{(2)} + \left(\Phi_b^0 - \Phi_e^0\right)(\cos\Phi_b^0)\alpha_b^{(3)} \right] = c_1, \tag{20d}$$

where the coefficients a_{11} and a_{12} are the same as in the first order problem, (17b,c), and c_1 is given in Appendix I.

The fifth equation needed to find $\phi_d^{(2)}$ and $\phi_s^{(2)}$ is the second order geometric compatibility (13), which becomes after the expressions for the second order forces, and for the second order rotation (these are given in [10]) are substituted

$$\begin{aligned} -\Phi_d^0 H\phi_d^{(2)} + \frac{D_s}{D_d}\Phi_s^0 h\phi_s^{(2)} &= \left[1 - \frac{\sin 2\Phi_d^0}{2\Phi_d^0} - \left(1 - \frac{\sin 2\Phi_s^0}{2\Phi_s^0} \right)\alpha_s^{(1)2} + \frac{2T}{\ell}\phi_d^{(1)}\cos\Phi_d^0 \right] \\ &\times \frac{EhH\ell^2}{8D_d} + \left[\phi_d^{(1)2} + \frac{\Phi_d^{02}}{8}\left(1 - \frac{\sin 2\Phi_d^0}{2\Phi_d^0} \right) \right]\frac{H}{2} \\ &- \left[\phi_s^{(1)2} + \frac{\Phi_s^{02}}{8}\left(1 - \frac{\sin 2\Phi_s^0}{2\Phi_s^0} \right)\alpha_s^{(1)2} \right]\frac{D_s h}{2D_d}. \end{aligned} \tag{20e}$$

The foregoing system of five linear equations (18a,b) and (20a,d,e) allows finding $\phi_d^{(2)}$, $\phi_s^{(2)}$, $\phi_e^{(2)}$, $\phi_b^{(2)}$ and $\alpha_b^{(3)}$, and hence the second order forces $P_d^{(2)}$, $P_s^{(2)}$ and the second order applied force $P^{(2)} = P_d^{(2)} + P_s^{(2)}$.

2.3. Displacements

Once the first and second order forces have been determined for the clamped-clamped case, the displacements can be found in the same manner as in [10]. For example, the mid-point deflection of the delaminated layer and that of the substrate part, can be found by integrating between the mid-point ($x = 0$) and the common interface ($x = \ell$)

$$w_{im} = 2\sin\left(\frac{\alpha_i}{2}\right)\sqrt{\frac{D_d}{P_d}}\left(\cos\Phi_i - 1\right). \tag{21a}$$

Substituting the asymptotic expansions for the force P_i and for the amplitude Φ_i, gives the mid-point displacement of the delaminated layer or the substrate part ($i = d, s$), as in [9], in the form

$$w_{im} = w_{im}^{(1)}\varepsilon + w_{im}^{(2)}\varepsilon^2 + \cdots. \tag{21b}$$

Finally, the previous analysis allows finding a direct expression for the applied strain ε_0 as follows

$$\varepsilon_0 L = \frac{P^0 L}{ET} + \left[\frac{P^{(1)}b}{ET} + \frac{P_d^{(1)}\ell}{Eh} + \frac{H}{2}\theta^{(1)}\right]\varepsilon + \left[\frac{f_d^{(2)}}{2} + \frac{P_d^{(2)}\ell}{Eh} + f_b^{(2)} + \frac{P^{(2)}b}{ET} + \frac{H}{2}\theta^{(2)}\right]\varepsilon^2 + \cdots. \tag{22}$$

3. Delamination growth characteristics

The initial postbuckling solution that has just been briefly described will now be used in conjuction with an interface crack solution. For the special case of a 'thin film' delamination, a fracture mechanics solution for the basic one-dimensional problem was given in [16]. The stress intensity factors or energy release rates depend on the ratio of delamination thickness over length h/ℓ. For $h/\ell \to 0$, these reduce to

$$K_{\mathrm{I}} = \left(c_1 P_m + c_2 \frac{M_m}{h}\right)\frac{1}{h^{1/2}}, \qquad K_{\mathrm{II}} = \left(c_3 P_m + c_4 \frac{M_m}{h}\right)\frac{1}{h^{1/2}},$$

where P_m and M_m are the force and moment at the mid-point of the delamination and

$$c_1 = 0.434, \qquad c_2 = 1.934, \qquad c_3 = 0.558, \qquad c_4 = -1.503.$$

These solutions were also used in the three-dimensional fracture analysis of thin-film debonding by Chai [17].

However, unlike these 'thin film' delamination papers, our present study imposes no restrictive assumptions on the relative delamination thickness or length. To this extent, we shall use the interface crack solutions summarized in [13], in the same manner as for the simply-supported case [10]. For a general bimaterial interface crack, these solutions depend on the Dundurs [18] parameters, $\tilde{\alpha}$, $\tilde{\beta}$ and the bimaterial constant $\tilde{\varepsilon}$. For the homogeneous system under consideration, $\tilde{\alpha} = \tilde{\beta} = \tilde{\varepsilon} = 0$. Therefore these formulas will be presented with the homogeneous material assumption taken into consideration.

For the plane-strain interface crack shown in Figure 1, the energy release rate G is

$$G = \frac{1-\nu}{4\mu}\left[\frac{P^{*2}}{Ah} + \frac{M^{*2}}{Ih^3} + 2\frac{P^* M^*}{\sqrt{AI}h^2}\sin\gamma\right], \tag{23a}$$

where μ is the shear modulus. P^* and M^* are linear combinations of the loads from the previous postbuckling solution

$$P^* = P_d - C_1 P - C_2 \frac{M_b}{h}, \tag{23b}$$

$$M^* = M_d - C_3 M_b. \tag{23c}$$

Moreover, A and I are positive dimensionless numbers and the angle γ is restricted such that $\gamma \leqslant \frac{1}{2}\pi$. These quantities as well as C_1, C_2 and C_3, depend only on the ratio h/H.

The preceding formula does not separate the opening and shearing components. Instead, the following two expressions give the mode I and mode II stress intensity factors

$$K_{\mathrm{I}} = \frac{1}{\sqrt{2}}\left[\frac{P^*}{\sqrt{Ah}}\cos\omega + \frac{M^*}{\sqrt{Ih^3}}\sin(\omega+\gamma)\right], \tag{24a}$$

$$K_{\mathrm{II}} = \frac{1}{\sqrt{2}}\left[\frac{P^*}{\sqrt{Ah}}\sin\omega - \frac{M^*}{\sqrt{Ih^3}}\cos(\omega+\gamma)\right]. \tag{24b}$$

Accurate determination of ω, which depends only on η (for a fixed set of Dundurs constants $\tilde{\alpha}$, $\tilde{\beta}$), requires the numerical solution of an integral equation and has been reported in [11]. The extracted ω, however, varies slowly with η in the entire range $0 \leqslant \eta \leqslant 1$, in accordance with the approximate formula [13]: $\omega = 52.1^\circ - 3^\circ\eta$. The mode mixity is defined by

$$\psi = \tan^{-1}(K_{II}/K_I). \tag{24c}$$

Substituting the asymptotic expressions for the forces and moments from the postbuckling solution already presented, gives

$$P^* = \varepsilon P^{*(1)} + \varepsilon^2 P^{*(2)} + \cdots, \qquad M^* = \varepsilon M^{*(1)} + \varepsilon^2 M^{*(2)} + \cdots, \tag{25a}$$

where the first and second order terms (i.e., $k = 1, 2$) are (notice that the zero order quantities in the expression for P^* cancel out)

$$P^{*(k)} = \frac{H}{T}P_d^{(k)} - \frac{h}{T}P_s^{(k)} - \frac{6hH}{T^3}M_b^{(k)}, \tag{25b}$$

$$M^{*(k)} = M_d^{(k)} - \frac{h^3}{T^3}M_b^{(k)}. \tag{25c}$$

In the previous relations, the first and second order forces and moments $P_d^{(k)}$, $P_s^{(k)}$, $M_d^{(k)}$, $M_b^{(k)}$, $k = 1, 2$ have already been found from the initial postbuckling solution described thus far.

Now the energy release rate and the mode I and II stress intensity factors can be written in the form

$$G = \varepsilon^2 G^{(2)} + \varepsilon^3 G^{(3)} + \cdots, \tag{26a}$$

$$K_{\mathrm{I,II}} = \varepsilon K_{\mathrm{I,II}}^{(1)} + \varepsilon^2 K_{\mathrm{I,II}}^{(2)} + \cdots. \tag{26b}$$

4. Discussion of results

The limiting, closed form solution for a very large value of the ratio h/T, i.e. for a delamination in an infinitely thick and infinitely long base plate subjected to an applied strain ε_0, is represented by the thin film model of Chai et al. [2]. Hence, by its assumptions, this solution is insensitive to the end conditions. The energy release rate predicted is expressed in terms of the Euler's critical strain for the delaminated layer ε_{cr} (treated as a column with built-in ends)

$$G(\varepsilon_0, \ell) = \tfrac{1}{2}Eh(1-\nu^2)(\varepsilon_0 - \varepsilon_{cr})(\varepsilon_0 + 3\varepsilon_{cr}); \qquad \varepsilon_{cr} = \frac{\pi^2 h^2}{12(1-\nu^2)\ell^2}. \tag{27a}$$

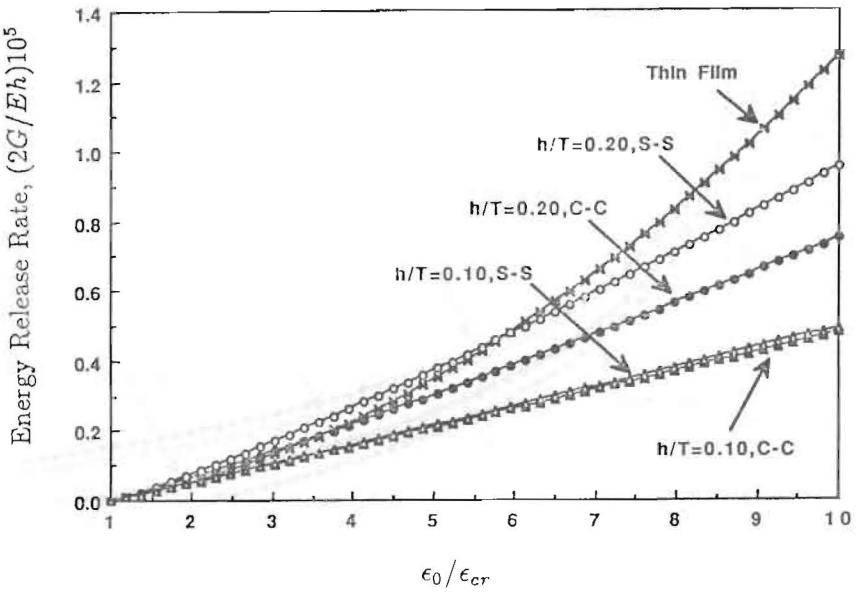

Figure 2. Energy release rate, $(2G/Eh)10^5$, as a function of the applied strain for both the clamped-clamped (C-C) and the simply-supported (S-S) cases.

For this model, the mode mixity is given by the following relation [13]

$$\tan\psi = \frac{4\cos\omega + \sqrt{3}\xi\sin\omega}{-4\sin\omega + \sqrt{3}\xi\cos\omega}; \qquad \xi = \left[\frac{4}{3}\left(\frac{\varepsilon_0}{\varepsilon_{cr}} - 1\right)\right]^{1/2}. \tag{27b}$$

For an illustration of the results from the previous analysis, consider a delaminated plate with $E = 10\,\text{GPa}$ and $\nu = 0.3$ and delamination and plate length $\ell = 20\,\text{mm}$ and $L = 60\,\text{mm}$, respectively, and delamination thickness $h = 0.4\,\text{mm}$. These dimensions correspond to our specimen dimensions (a width of 10 mm has also been considered and is appropriately accounted for in the results). To keep the critical strain ε_{cr} constant, we keep the delamination length and thickness constant and vary only the plate thickness to get a varying ratio h/T; this would ensure the same thin film model solution.

Figure 2 shows the energy release rate $(2G/Eh)10^5$, as a function of the applied strain for $h/T = 0.10$ and $h/T = 0.20$ for both the clamped and simply-supported cases. It is seen that for the same applied strain, the effects of the end conditions are found to depend on the relative location of the delamination through the thickness. Specifically, delaminations located closer to the surface, $h/T = 0.10$, exhibit nearly the same energy release rate either in a clamped-clamped or a simply supported configuration. However, in delaminations located further away from the surface, $h/T = 0.20$, there is a marked difference, the energy release rate being larger in the simply-supported case. The same major trend that has been observed in the simply supported case, i.e. the increased growth resistance of the delaminations located near the surface relative to the ones located further inside the plate, is also observed in the clamped-clamped case. Specifically, a larger energy release rate is found to be present during the initial postbuckling phase for the delaminations of increasing ratio of delamination thickness over plate thickness, $h/T = 0.20$ (i.e. delaminations further away from the surface) in comparison with the ones closer to the surface, $h/T = 0.10$. Experimental results on clamped delaminated

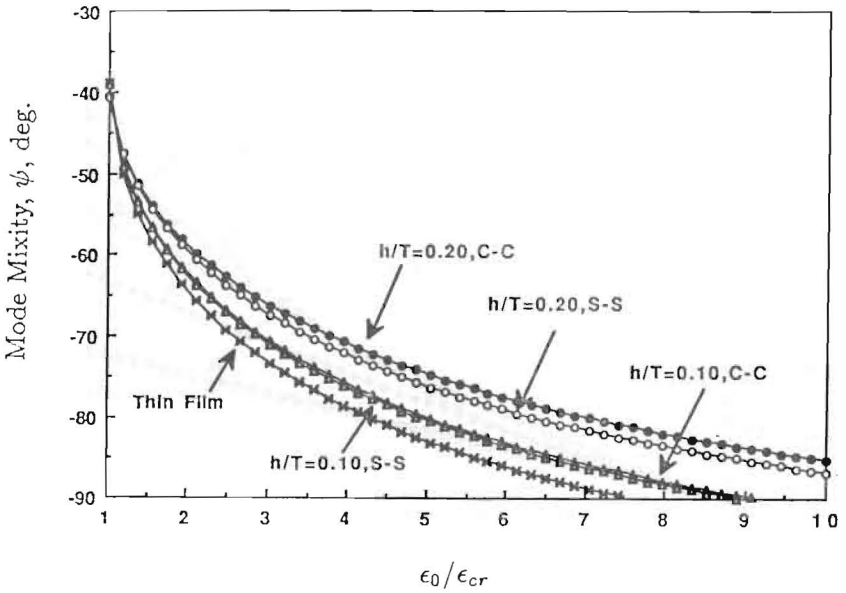

Figure 3. Mode mixity ψ^0 versus applied strain for both the clamped-clamped (C-C) and the simply-supported (S-S) cases.

plates that have been previously reported by Kardomateas [19–20] confirm clearly the reduced growth resistance of the 'large ratio' (deeply located) delaminations, versus the 'small ratio' ones.

Notice that in the beginning, i.e. for relatively small applied strain, the curves tend toward the thin film solution for a decreasing ratio h/T (as expected); however as the applied strain is increased, the thin film model solution rises at a fast pace and predicts a much higher energy release rate.

Another very interesting result is the variation of the mode mixity (mode II versus mode I) at the delamination tip. Figure 3 shows the mode mixity ψ versus applied strain. Again, it is seen that delaminations located closer to the surface, $h/T = 0.10$, exhibit nearly the same mode mixity either in a clamped-clamped or a simply supported configuration. However, in delaminations located further away from the surface, $h/T = 0.20$, there is a noticable difference; a higher mode II component exists in the simply-supported case.

The major trend of a higher mode I component in the delaminations located further away from the surface, $h/T = 0.20$, than the ones closer to the surface, $h/T = 0.10$, is again observed in the clamped-clamped case. Notice that the thin film model predicts a higher mode II component in all cases and that the value of the applied strain at which the delamination tip loading becomes pure mode II ($\psi = -90^0$) is at $\varepsilon_0/\varepsilon_{cr} = 7.55$.

Figure 4 shows the mid-point deflection of the delamination w_{dm}/h and Figure 5 shows the mid-point deflection of the substrate part w_{sm}/h both as a function of the applied strain. The mid-point transverse displacement of the delaminated layer as well as that of the substrate part, is clearly larger in the simply supported case for $h/T = 0.20$, i.e. for delaminations located further away from the surface, but nearly the same for delaminations near the surface, $h/T = 0.10$. The difference between the clamped-clamped and the simply supported cases for $h/T = 0.20$ is particularly noticeable for the mid-point displacement of the substrate

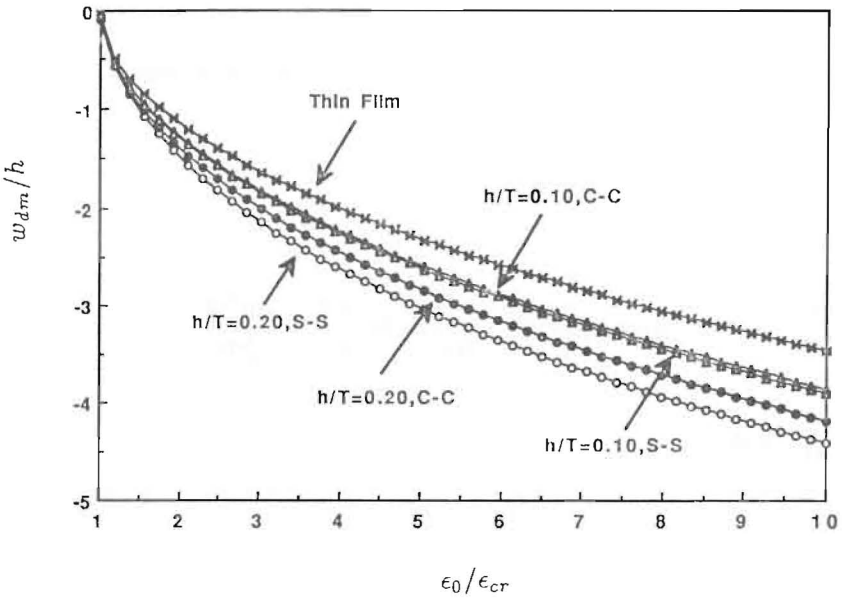

Figure 4. Mid-point deflection of the delamination w_{dm}/h as a function of the applied strain for both the clamped-clamped and the simply-supported cases.

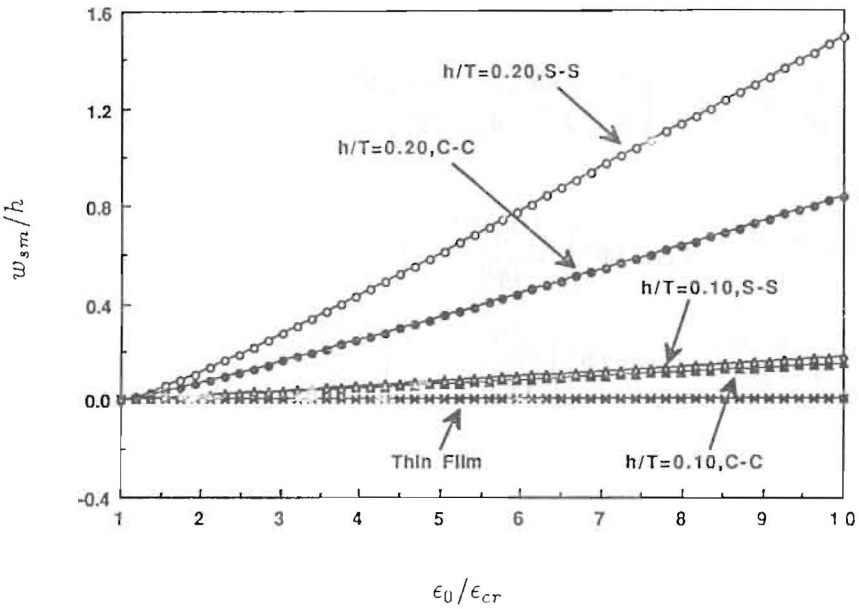

Figure 5. Mid-point deflection of the substrate part w_{sm}/h versus applied strain for both the clamped-clamped and the simply-supported cases.

(Figure 5). Both curves for both end conditions show a trend toward the thin film solution for a decreasing ratio h/T and the mid-point deflections are always higher for a larger value of h/T (delaminations located further away from the surface).

Appendix I

The constant c_1 in (20d) is given as follows (it includes terms from the expressions of $M_d^{(3)}$, $M_s^{(3)}$ and $M_b^{(3)}$)

$$c_1 = \frac{D_d}{\ell} c_{1d} + \frac{D_s}{\ell} c_{1s} + \frac{D_b}{b} c_{1b} + c_{1c}, \tag{A1}$$

where

$$c_{1d} = \left(\frac{\Phi_d^0}{2} \cos \Phi_d^0 + \sin \Phi_d^0 \right) \phi_d^{(1)2} - \frac{\Phi_d^0}{16} \cos \Phi_d^0 \left(\frac{1}{3} - \frac{\sin 2\Phi_d^0}{2\Phi_d^0} \right), \tag{A2a}$$

$$\begin{aligned} c_{1s} = {} & \alpha_s^{(1)} \left[\left(\frac{\Phi_s^0}{2} \cos \Phi_s^0 + \sin \Phi_s^0 \right) \phi_s^{(1)2} - \frac{\Phi_s^0}{16} \cos \Phi_s^0 \left(\frac{1}{3} - \frac{\sin 2\Phi_s^0}{2\Phi_s^0} \right) \alpha_s^{(1)2} \right] \\ & - \left(\cos \Phi_s^0 - \Phi_s^0 \sin \Phi_s^0 \right) \phi_s^{(1)} \alpha_s^{(2)} - \gamma_c \Phi_s^0 \cos \Phi_s^0, \end{aligned} \tag{A2b}$$

$$\begin{aligned} c_{1b} = {} & - \left[q\phi_b^{(1)} - (\cos \Phi_b^0) \phi_e^{(1)} \right] \alpha_b^{(2)} \\ & + \left[\phi_b^{(1)} \left(\phi_b^{(1)} - \phi_e^{(1)} \right) \sin \Phi_b^0 + \left(\Phi_b^0 - \Phi_e^0 \right) (\cos \Phi_b^0) \frac{\phi_b^{(1)2}}{2} \right] \alpha_b^{(1)} \\ & - \frac{1}{16} \left(\Phi_b^0 - \Phi_e^0 \right) \left(\frac{1}{3} - \frac{1}{2} \frac{\sin 2\Phi_b^0 - \sin 2\Phi_e^0}{\Phi_b^0 - \Phi_e^0} \right) (\cos \Phi_b^0) \alpha_b^{(1)3}, \end{aligned} \tag{A2c}$$

and

$$\begin{aligned} c_{1c} = {} & \left[\left(\frac{\sin 2\Phi_s^0}{\Phi_s^0} - 2 \cos 2\Phi_s^0 \right) \frac{\phi_s^{(1)} \alpha_s^{(1)2}}{4\Phi_s^0} + \left(1 - \frac{\sin 2\Phi_s^0}{2\Phi_s^0} \right) \alpha_s^{(1)} \alpha_s^{(2)} - \right. \\ & \left. - \left(\frac{\sin 2\Phi_d^0}{\Phi_d^0} - 2 \cos 2\Phi_d^0 \right) \frac{\phi_d^{(1)}}{4\Phi_d^0} - \frac{\psi_d T}{\ell} \right] \frac{EhH}{4}. \end{aligned} \tag{A2d}$$

Acknowledgement

The financial support of the Office of Naval Research, Ship Structures and Systems S&T Division, Grant N00014-91-J-1892, and the interest and encouragement of the Grant Monitor, Dr. Y.D.S. Rajapakse, are both gratefully acknowledged.

References

1. G.A. Kardomateas and D.W. Schmueser, *AIAA Journal* 26 (1988) 337–343.
2. H. Chai, C.D. Babcock and W.G. Knauss, *International Journal of Solids and Structures* 17 (1981) 1069–1083.
3. G.J. Simitses, S. Sallam and W.L. Yin, *AIAA Journal* 23 (1985) 1437–1444.
4. S.S. Wang, N.M. Zahlan and H. Suemasu, *Journal of Composite Materials* 19 (1985) 296–316.
5. A.G. Evans and J.W. Hutchinson, *International Journal of Solids and Structures* 20 (1984) 455–466.

6. H. Chai and C.D. Babcock, *Journal of Composite Materials* 19 (1985) 67–97.
7. I. Vardoulakis and E. Papamichos, *International Journal of Rock Mechanics, Mineral Science and Geomechanics Abstracts* 28 (1991) 163–173.
8. G.A. Kardomateas, *AIAA Journal* 27 (1989) 624–631.
9. I. Sheinman and M. Adan, *Journal of Applied Mechanics (ASME)* 54 (1987) 558–562.
10. G.A. Kardomateas, *Journal of Applied Mechanics (ASME)* 60 (1993) 903–910.
11. Z. Suo and J.W. Hutchinson, *International Journal of Fracture* 43 (1990) 1–18.
12. K.-F. Nilsson and B. Storåkers, *Journal of Applied Mechanics (ASME)* 59 (1992) 530–538.
13. J.W. Hutchinson and Z. Suo, in *Advances in Applied Mechanics*, Academic Press, vol. 29 (1992) 63–191.
14. S.J. Britvek, *The Stability of Elastic Systems*, Pergamon, New York (1973).
15. M.J.D. Powell, in *Numerical Methods for Nonlinear Algebraic Equations*, P. Rabinowitz (ed.), Gordon and Breach, New York (1970) 87-161.
16. M.D. Thouless, A.G. Evans, M.F. Ashby and J.W. Hutchinson, *Acta Metallurgica* 35 (1987) 1333–1341.
17. H. Chai, *International Journal of Fracture* 46 (1990) 237–256.
18. J. Dundurs, *Mathematical Theory of Dislocations*, American Society of Mechanical Engineering, New York (1969) 70–115.
19. G.A. Kardomateas, in *Interlaminar Fracture in Composites*, 'Key Engineering Materials' series, Trans Tech Publications, Ltd., Switzerland (1989) 269–284.
20. G.A. Kardomateas, *Journal of Composites Technology and Research (ASTM)* 12 (1990) 85-90.